# A Study of Thermodynamically Favorable Crystals in Branched Polymers: A Disentangled and Crystallizable Interphase

**Ankur Rastogi, Ann E. Terry, Vincent B. F. Mathot, and Sanjay Rastogi***

*Department of Chemical Engineering/The Dutch Polymer Institute, Eindhoven University of Technology, P.O. Box 513, 5600MB Eindhoven, The Netherlands*

*Received September 24, 2004; Revised Manuscript Received February 11, 2005*

ABSTRACT: The paper addresses the crystallization behavior of homogeneous branched polyethylenes, where the branches cannot be incorporated within the lattice. The polymer was chosen to investigate the morphology achievable by polymers where the chains cannot extend, which is considered to be a requisite to minimize the surface free energy. Pressure−temperature conditions similar to those necessary to form extended chain crystals in linear polyethylenes are applied. In-situ wide-angle X-ray diffraction and Raman spectroscopy are used to follow the structural and conformational changes during crystallization. The hexagonal phase is not observed in these polymers unlike in linear polyethylene. However, crystallization at elevated pressures results in a structural organization of the interphase and the fold surface; this provides adjacent reentry, where the branches will also possess structural order. Crystallization of these components leads to the formation of an incompressible open-orthorhombic phase ($a = 7.56$ Å, $b = 5.03$ Å, $c = 2.55$ Å, density = 960 kg/m$^3$) in addition to the existing orthorhombic crystalline domain. With the crystallization of the chains at the interphase and on the fold surface, a contraction in the parent orthorhombic phase or its transformation into the monoclinic phase is observed. Our experimental data suggest that in such a class of polymers the thermodynamically stable state will be crystals with an ordered interphase that can be achieved ultimately by disentanglement of the chains in the amorphous region. The disentangled nature of the amorphous component is further supported by solid-state mechanical deformation of samples.

## Introduction

The semicrystalline structures often formed by crystallizable polymers are known to consist of thin crystalline lamellae separated by amorphous regions.[1−5] For crystallization from the melt, where the conditions are far from equilibrium, the polymer chains must achieve a regular conformation from the highly entangled melt and align parallel to each other to form thin platelike lamellae, the entanglements being confined to the amorphous regions. It is still unclear whether the polymer chains do actually disentangle or merely that during crystallization entanglements are pushed to the surface.[6] However, independent of the mechanism involved, the molecular structure of the amorphous region is dictated by the crystallization conditions, either in the presence of flow or not, as well as by the chemical nature and inherent shape of the polymer. Experimental efforts to decouple the mechanical properties of polymers from the crystalline and amorphous fractions have not been particularly successful because of this dependence of the molecular organization in the amorphous region upon the crystallization conditions. Moreover, a third structural component, an interphase of intermediate order, could exist between the amorphous and crystalline phases, as has been proposed both theoretically and experimentally, which means that a sharp demarcation line between the amorphous and crystalline phases is unlikely. This added complication is necessary if one considers that the chains emerge at the crystalline surfaces with a high degree of molecular alignment. These chains must either fold back into the crystal, perhaps by adjacent reentry, or reside in the amorphous matrix. In the case of crystallization from the melt, where the crystallization conditions are often very far from equilibrium, extensive and perfect folding will strongly depend on molecular weight and molecular architecture and in most cases will be highly improbable. Assuming the crystalline domains are sufficiently large in the basal plane, then at small distances away from each crystalline domain most of the chains present will have originated from the crystal surface. The average chain orientation here will not be random as in the bulk amorphous matrix but will be distributed around the normal to the crystal surface: this is the proposed semiordered interfacial component, the degree of ordering strongly depending upon the crystallization conditions. In several cases this may also give rise to a crystallographic registry and influence further the physical and mechanical properties of the polymer.

Controversy still surrounds the existence of this "interphase". Increasingly experimental evidence is appearing in the literature to support its existence; terms to describe it include "semi-ordered", "intermediate", "rigid amorphous", "interfacial", "interzonal", "interphase", and "transitional zone" and give quite a clear picture of what is envisaged. A comprehensive review has been compiled by Mandelkern[7] and has been further supported by WAXD studies by Windle.[8] Using off-lattice Monte Carlo simulations, Rutledge and coworkers[9] have reported a recent detailed study on the interphase with different degrees of chain tilt.

The basis for our work is examining the structural order present in the interphase and its influence on the crystalline domain as well as mechanical properties. Pressure has proven to be an important thermodynamic component in polymer crystallization: it shifts the Gibbs free energy of the system and thus increases the melting temperature following the simple principle

* Corresponding author. E-mail: s.rastogi@tue.nl.

10.1021/ma048023b CCC: $30.25 
Published on Web 05/05/2005

$(\partial G/\partial p)_{liquid} > (\partial G/\partial p)_{crystal}$. The increase in melting temperature enhances the overall chain mobility and thus facilitates the process of segregation of the chains of similar configuration or molar mass.[10] By exploiting the effects of pressure on crystallization, it might be feasible to segregate chains according to ethylene sequence length distribution in homogeneous ethylene−octene copolymers. It is well-known that when linear polyethylene is crystallized at elevated pressures, extended chain crystals are formed due to the intervention of the hexagonal phase.[11,12] However, in homogeneous branched polyethylenes, Bassett et al. have concluded from detailed morphological studies that the anticipated hexagonal phase is absent at high pressures and temperatures.[13] In this paper in-situ wide-angle X-ray diffraction of homogeneous ethylene−octene copolymers at elevated pressures and temperatures is performed.

We already know that pressure enables us to achieve a well-defined morphology in branched alkanes.[14] At atmospheric pressure, butyl- and methyl-branched alkanes exhibit similar crystallographic behavior to linear alkanes and linear polyethylene: orthorhombic packing is maintained even though the branches will be excluded to the lamellar surface. For the nascent sample, as obtained on synthesis, the lamellar spacing corresponds to chains that are once-folded with the butyl branches excluded to the surface and chains perpendicular to the basal plane, i.e., the chains are not tilted. Upon heating, some of the chains begin to tilt with a chain tilt angle of approximately 35°, and upon cooling this tilted structure is retained. Noninteger folds were not observed.

Figure 1a reiterates an essential finding of our previous work[14] for the pressure−temperature path adopted as shown in the inset. Initially upon crystallization from the melt, the butyl-branched alkanes crystallize directly in the orthorhombic phase. The figure shows that the orthorhombic (110) and (200) reflections gain intensity upon cooling, and a weak monoclinic reflection appears at approximately 148 °C. These reflections have been assigned considering the earlier work by Hay and Keller.[15] With subsequent cooling to ∼70 °C, a relatively broad and weak new reflection at $d = 4.2$Å appears next to the monoclinic reflection, which was assigned as the "pseudohexagonal" phase. The appearance of the new reflection is followed by an increase in the intensity of the monoclinic reflection with a simultaneous sudden drop in the intensity of the orthorhombic reflections and a shift to higher angles, implying a densification of the orthorhombic crystalline lattice ($\rho = 1141$ kg/m$^3$ at 4.0 kbar, 25 °C).

It is remarkable that, unlike the monoclinic and orthorhombic phases, the pseudohexagonal phase does not show any expansion or contraction with temperature (Figure 1a) or pressure (Figure 1b), since the pseudohexagonal phase arises from the crystallization of the interphase (or the fold surface when chains fold by adjacent reentry). The interphase as well as butyl branches present on the fold surface crystallize on compression (or cooling) and loses the order on releasing pressure (or heating). Figure 1b shows that concomitant to the disappearance of the pseudohexagonal phase a sudden expansion in the orthorhombic phase occurs, which is followed by the solid−solid transformation of the monoclinic phase into the orthorhombic phase. These results demonstrate that the contraction of the orthorhombic lattice and appearance of the monoclinic phase are linked with the crystallization of the interphase and the butyl branches present on the fold surface.

If the response of methyl branched alkanes to the same pressure−temperature path adopted for butyl-branched alkanes is examined (Figure 2) on cooling at elevated pressures from the melt, part of the orthorhombic phase goes into the monoclinic phase without the appearance of any new reflections. The orthorhombic lattice is seen to contract. Absence of any new reflections must be due to the shorter length of the methyl branches as compared to the longer length of the butyl branches, which, although the methyl branches may be organized on the fold surface, their length precludes them from cocrystallization.

One of the significant features from the above experiments on model, well-defined branched alkanes is that pressure facilitates the formation of a structured morphology, where branches on the crystal surface also show crystallographic registration if they are of sufficient length to crystallize. When given appropriate conditions, due to the increased chain mobility in the melt, large crystals having well-ordered branches on the *ab* plane of the crystal can be obtained. Although the chains are not likely to be extended, as would be anticipated for linear polyethylenes from the conventional theories, the crystal thickness defined by the distribution of the branches appears to be the thermodynamically most favorable state that is achievable kinetically with pressure.

Taking these observations into account, and to explore the generality of the observations for these model systems, homogeneous ethylene−octene copolymers, which also cannot form extended chain crystals because of the exclusion of the hexyl branches from the crystal lattice, have been chosen for our studies. One of the main characteristics of these copolymers is that they are "homogeneous" copolymers as there is no difference in comonomer distribution along the chains other than differences related to statistical fluctuations.[16] Homogeneous copolymers are synthesized with the aid of a single set of reactivity values, corresponding to a single active catalyst site, resulting in a single peaked ethylene sequence length distribution (ESLD). In contrast, copolymers such as LLDPE are considered to be heterogeneous and show a superposition of multiple ESLDs, as the synthesis involves the presence of two or more active catalyst sites. Crystallization kinetics and the subsequent morphology are strongly influenced by the specific chain microstructure—specifically the ESLD, which varies with the mol % of octene. In the case of ethylene−1-octene copolymers, the chain microstructure greatly affects the properties since the ethylene units will form crystalline domains, while the hexyl units are likely to be excluded from the domains. Therefore, the exact distribution of the comonomer units along the chain, and consequently the way of stringing together of the ethylene sequences, determines the crystallizability of that chain. As is evident, the chain microstructure will also influence the chain conformation in the melt and in the solution because the bond angles of the monomers and comonomers will differ.

In ethylene−1-octene copolymers, the phase behavior is more complicated at elevated pressures and has been little studied. High pressures and temperatures lead to extended ethylene sequence crystals (EESCs), rather than extended chain crystals (EECs); the chain sequence

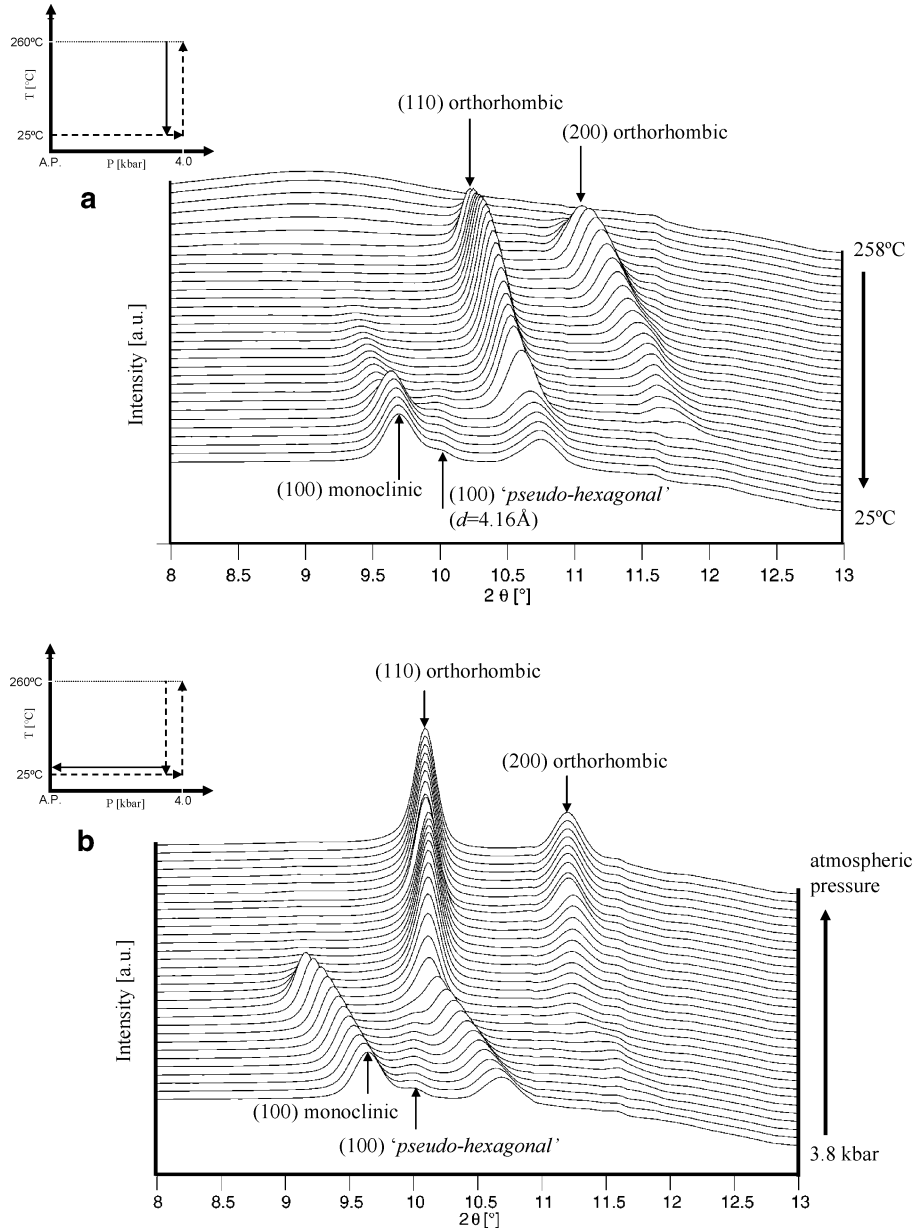


**Figure 1.** (a) Crystallization of butyl-branched alkane ($C_{96}H_{193}CH(C_4H_9)C_{94}H_{189}$) from the melt at 4.0 kbar is shown with a series of integrated WAXD patterns recorded while cooling at a rate of 4 °C/min (inset shows the pressure temperature cycle to which the sample was subjected; X-ray wavelength, $\lambda = 0.744$ Å). The orthorhombic (110) and (200) reflections appear first and gain in intensity with increasing supercooling. A weak (100) monoclinic reflection appears at ~148 °C. Upon further cooling to below 70 °C, the "pseudohexagonal" phase forms. On continuing to cool, there is a further increase in the intensity of the (100) monoclinic reflection and a simultaneous contraction of the orthorhombic lattice. (b) A series of WAXD integrations showing that, upon releasing pressure at room temperature (i.e., following solid line in inset) for the sample as crystallized in (a), the monoclinic and orthorhombic reflections move to lower angles while the "pseudohexagonal" reflection stays at $d = 4.16$ Å. The orthorhombic lattice does not expand any further once the pseudohexagonal phase disappears. This is followed by the solid−solid transformation from monoclinic to orthorhombic phase at lower pressures.

can only extend between branching points if the polymer chain mobility is high enough. By high-pressure DSC, Vanden Eynde et al.[17] showed that the melting and crystallization transitions are shifted to higher temperatures due to a shift in the Gibbs free energy of the melt with increasing pressure. For low 1-octene comonomer content, three processes were suggested: the melting of folded chain crystals, followed by the melting of the relatively large EECs/EESCs superimposed on the orthorhombic to hexagonal transition and a high-temperature melting of the hexagonal phase. The lack of convincing experimental evidence needs to be addressed by in-situ high-pressure X-ray studies.

## Experimental Section

**Materials.** The experiments were performed on a homogeneous ethylene−1-octene copolymer with 5.2 mol % comonomer content ($M_w = 31\,000$ g/mol). The average short chain branching content (SCBC)/1000 carbon atoms is 22.5, and the polydispersity is approximately 2. The samples were melt-pressed at 150 °C to a thickness of 0.4 mm and left for 5 min at that temperature. They were cooled subsequently to room temperature with a cold−water circulation around the press at a rate of approximately 30 °C/min at atmospheric pressure. The samples used for WAXD and Raman spectroscopy studies had the same thermal history. The samples for mechanical testing were prepared using a large-volume pressure vessel where the temperature and pressure could be controlled for a

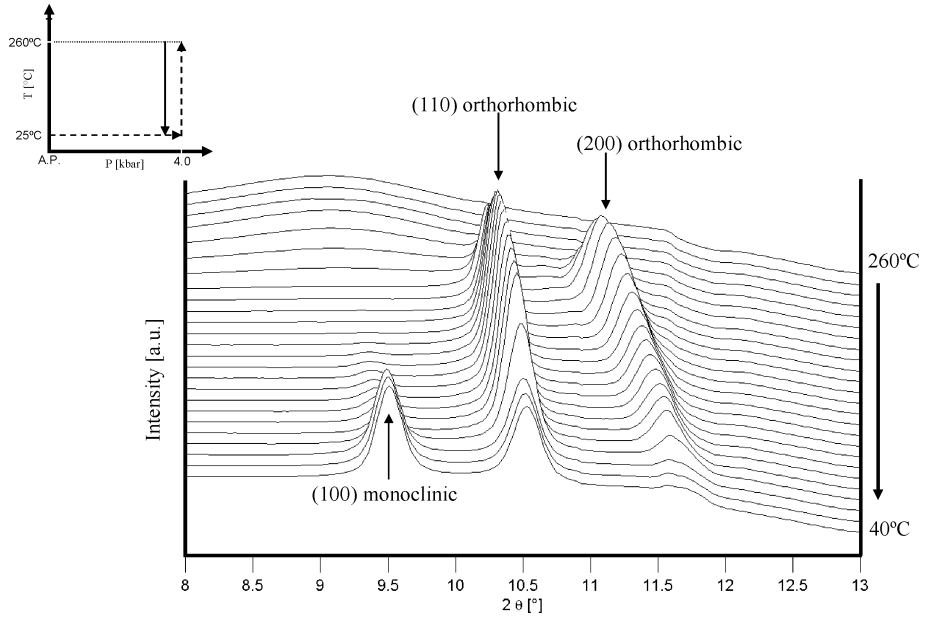


**Figure 2.** Crystallization of methyl-branched alkane $C_{96}H_{193}CH(CH_3)C_{94}H_{189}$ is shown in a series of WAXD patterns at ~4.0 kbar. During cooling from 260 °C, the sample initially crystallizes in the orthorhombic phase. A weak monoclinic reflection appears at ~140 °C accompanied by a small drop in intensity of the (110) and (200) orthorhombic reflections. At 65 °C, the intensity of the (100) monoclinic reflection greatly increases at the expense of the orthorhombic reflections. No new reflection is observed unlike in the case of butyl-branched alkane depicted in Figure 1.

sufficiently large sample volume to make dumbbell-shaped samples for tensile tests or cylindrical samples for compression. Experimental conditions for mechanical tests were similar to those described elsewhere.[23]

**Equipment.** The high-pressure experiments were carried out using a piston cylinder type pressure cell, similar to the one designed by Hikosaka and Seto.[18] The maximum attainable pressure in the current setup is 5.0 kbar. The temperature can be varied from room temperature to 300 °C. A sample of 0.4 mm thickness is placed in between two diamonds windows, each having a thickness of 1 mm, and surrounded by Teflon spacer rings. The use of diamond windows allows in-situ X-ray diffraction studies to be performed in transmission through the sample. For the purpose of Raman spectroscopy, sapphires were used instead of diamond windows to reduce the interference of the otherwise strong phonon vibration around 1350 $cm^{-1}$ (due to the diamond window) with the $CH_2$ twisting mode of polyethylene. Pressure on the sample is generated with the relative movement of two pistons activated by regulated nitrogen gas. It is to be noted that nitrogen gas does not come in contact of the sample. The smooth motion of the pistons keeps constant pressure throughout the experiments.

In-situ wide-angle X-ray diffraction measurements were performed using monochromatic X-rays of wavelength 0.744 Å at the Materials Science beamline ID11, European Synchrotron Radiation Facility (ESRF), Grenoble, France. The high flux and relatively low wavelength were required to overcome X-ray absorption by the diamond windows within the pressure cell. Each diffraction pattern was exposed for 25 s on a two-dimensional CCD detector. The delay time was adjusted to record two diffraction patterns every minute. The data were corrected for spatial distortion of the detector using the pattern from a specific calibration grid placed on the front of the detector. The circular coordinates of strong reflections were used to determine the beam center. The two-dimensional X-ray patterns were transformed into one-dimensional plots by performing integration against $2\theta$ using FIT2D (ESRF). Silicon standard (NIS 620b) was used to calibrate the exact sample-to-detector distance and Bragg $d$ values for the various crystalline reflections.

In-situ high-pressure Raman spectroscopy was performed using a Labram spectrometer from Dilor S.A. (France). A Spectra Physics Millennium II Nd:YVO4 laser at 532 nm was used as the excitation source. The initial power was 0.20 W. Laser light was focused onto the sample using a slit width of 100 $\mu$m and a 20× microscope objective. The exposure time for each spectrum was 10 s followed by a delay time of 20 s so that two spectra were recorded every minute. The backscattered light from the sample was dispersed with an 1800 $mm^{-1}$ grating on the CCD detector. The analysis of the Raman spectra involved baseline correction, and the spectra were normalized to the intensity of the internal standard band at 1295 $cm^{-1}$.

## Results and Discussion

The sample used for our studies is an ethylene−1-octene copolymer having 5.2 mol % of octene. The molecular characteristics of the sample are described in the Experimental Section. The starting condition for each experiment is a sample cooled at 10 °C/min from the melt at atmospheric pressure, for which the WAXD pattern shows an unoriented orthorhombic phase (Figure 3a). On compression at room temperature to a pressure of 3.7 kbar, although there is an increase in the intensity of the monoclinic (100) reflection, a considerable loss in crystallinity is observed with the disappearance of the orthorhombic (110) and (200) reflections and the appearance of the amorphous halo. It is to be noted that no global orientation on compression is observed although the monoclinic phase is often associated with shear. The whole process of apparent amorphization on compression is fully reversible with releasing pressure. At first glance the amorphization may appear similar to the solid-state amorphization reported earlier in poly(4-methylpentene-1).[19] To examine changes at the molecular level, in-situ high-pressure Raman spectroscopy has been performed. Figure 3b shows room temperature Raman spectra of the same sample recorded at atmospheric and elevated pressures (3.9 kbar). The spectrum at atmospheric pressure is representative of a typical vibrational mode for the orthorhombic crystals. The triplet within the region 1400−1500 $cm^{-1}$ is specific to the splitting of the vibrational modes of the polyethylene chains packed in the orthorhombic unit cell. With the application of

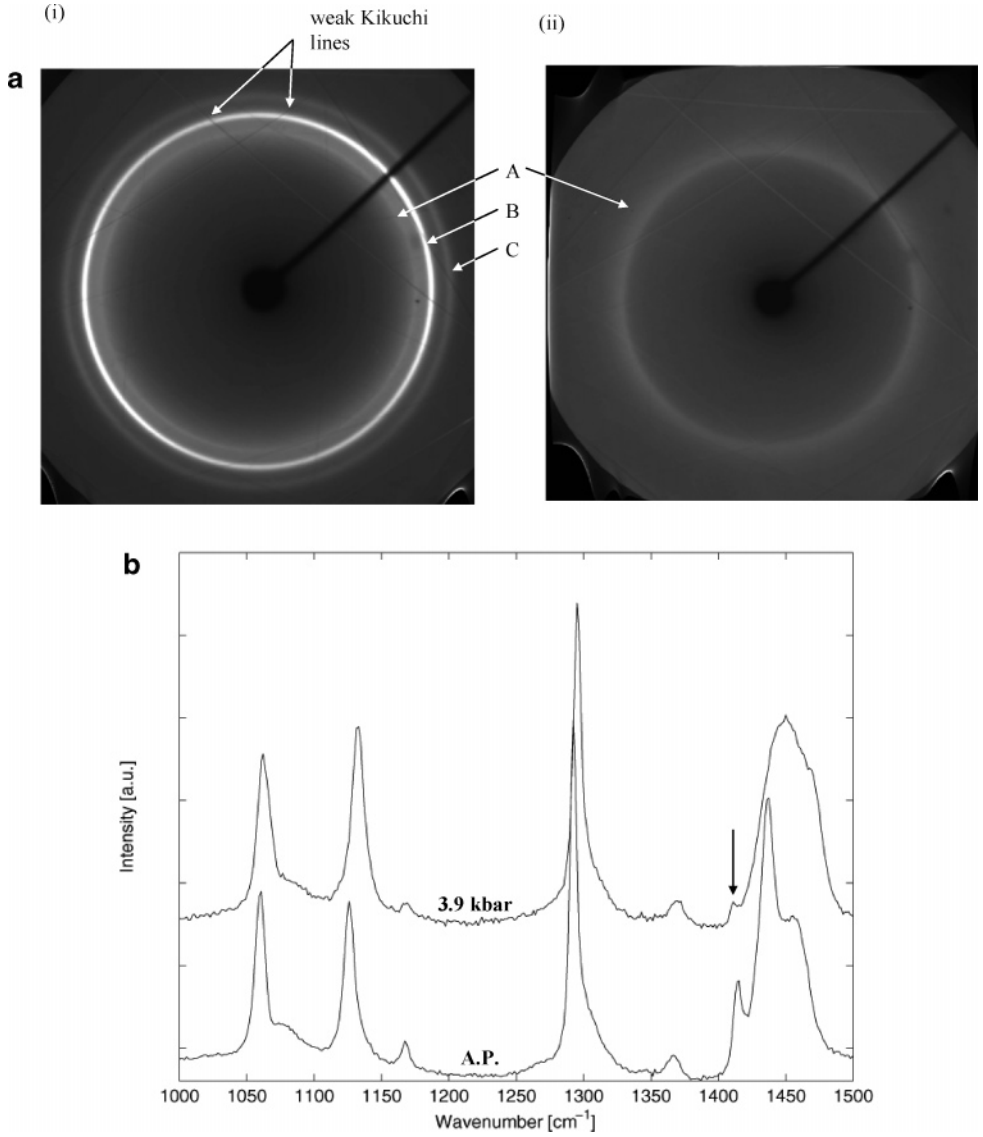


**Figure 3.** (a) Two-dimensional WAXD diffraction patterns of ethylene−1-octene copolymer (5.2 mol %) in the pressure cell recorded at room temperature are shown. Weak Kikuchi lines are seen which arise from the diamond windows of the pressure cell. (i) Taken at atmospheric pressure: while majority of the crystals are in the orthorhombic phase, a weak monoclinic phase appears due to shear during the loading of the sample [A: (100) monoclinic; B: (110) orthorhombic; C: (200) orthorhombic]. (ii) The same sample at 4.0 kbar: the diffuse halo suggests that the sample becomes "amorphous" at these high pressures. The orthorhombic reflections disappear, leaving behind weak monoclinic phase and "apparent" amorphous phase. (b) Comparison of in-situ Raman spectra recorded at room temperature of ethylene−1-octene copolymer (5.2 mol %) at atmospheric pressure and at 3.9 kbar. The same pressure cell was used as for the in-situ X-ray experiments with the diamonds windows replaced by sapphire.

pressure, the 1415 cm$^{-1}$ vibrational mode associated with the orthorhombic phase[20] shows a remarkable decrease in intensity. This could be explained by the loss of crystallinity and appearance of the symmetric nature of the vibrational modes in the monoclinic phase.[21] This observation is in accordance with the WAXD pattern recorded at elevated pressures; a closer examination of the Raman spectra clearly demonstrates no change in the trans or the appearance of a gauche component. This suggests that the disappearance of the orthorhombic reflections in the WAXD pattern is due to a reduction in the long range order, while the short-range conformational order is maintained. The broadening of peaks in the triplet region is characteristic of high pressures, which occurs due to the restricted vibrational motion in the confined space. We would like to state that the apparent amorphization in ethylene−octene copolymers is thus considerably different than the solid-state amorphization in poly(4-methylpentene-1), where in the latter large conformational changes were observed with the loss in crystallinity.[19]

The copolymer in the apparently amorphous state was heated at a rate of 2 °C/min, isobarically at 4 kbar. On heating, close to 120 °C, the monoclinic phase transforms into the orthorhombic phase, and the amorphous fraction crystallizes. After completely melting, the sample was cooled slowly at a rate of 2 °C/min. The slow heating/cooling rates were chosen to provide enough time for the various ethylene sequences lengths to segregate. Crystallization from the melt occurs directly into the orthorhombic phase without the intervention of the hexagonal phase at these high pressures and temperatures. Figure 4a shows that on cooling further, below 100 °C, a new reflection appears at a lower angle, corresponding to a Bragg spacing of 4.19 Å. The new reflection intensifies on further cooling, and a secondary relatively weak new reflection becomes evident at a $d$-spacing of 3.78 Å. It is to be noted that the amorphous

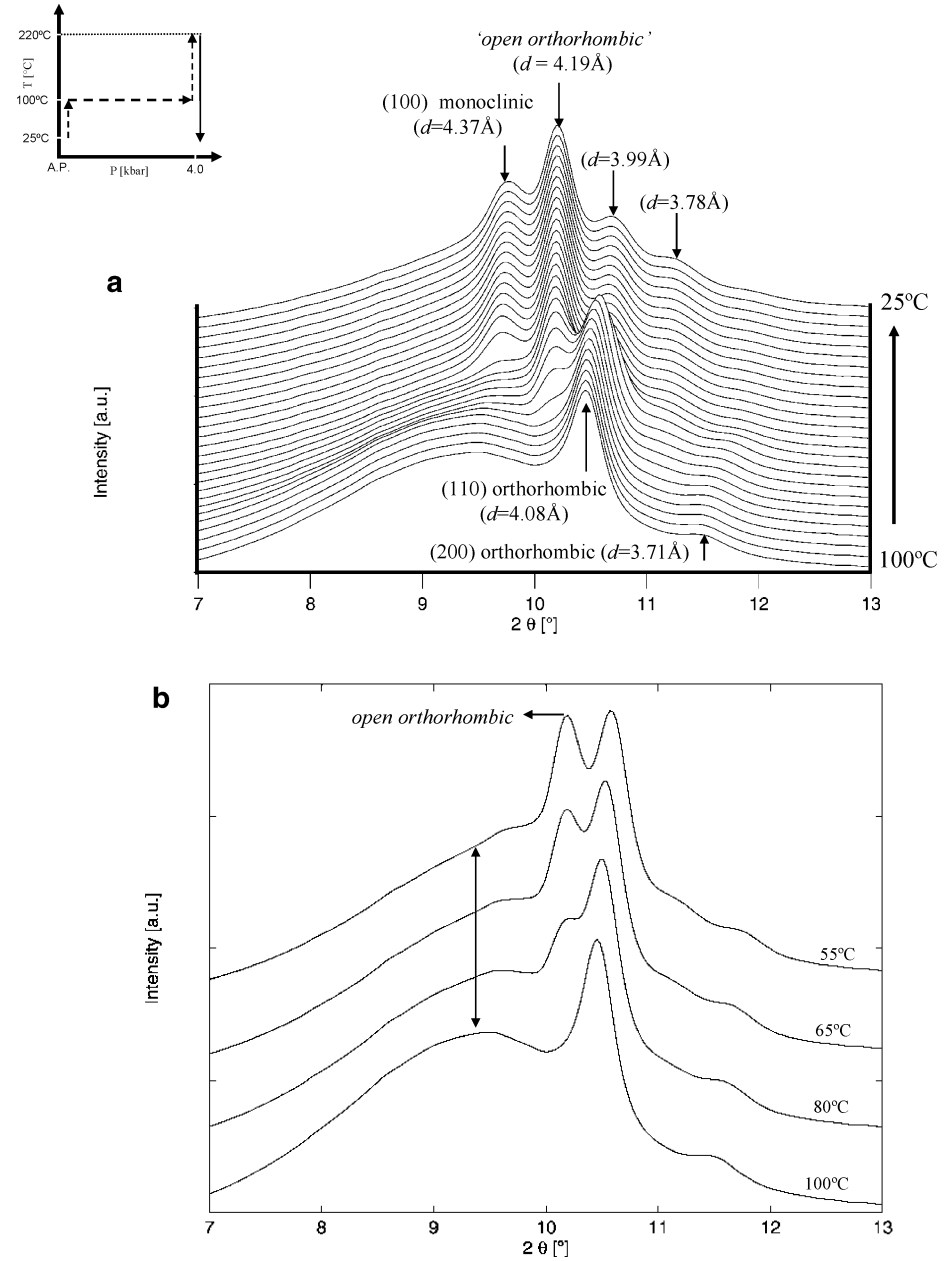


**Figure 4.** (a) Diffraction patterns of ethylene−1-octene copolymer (5.2 mol %) shown for temperature from 100 to 25 °C, upon cooling from the melt at ∼3.8 kbar. The open-orthorhombic phase appears at ∼80 °C. This is followed by the appearance of the (100) monoclinic reflection concomitant with a shift to higher angles and a drop in the intensity of the parent orthorhombic reflections. Inset shows the pressure−temperature cycle adopted for the experiments. (b) A selection of WAXD patterns showing in detail the appearance of the open-orthorhombic phase with a drop in the amorphous content. The intensity of the parent orthorhombic phase remains unaltered.

content decreases with the appearance and intensification of the new reflections. This has been shown explicitly in Figure 4b. Another salient feature in the figure is a sudden decrease in the intensity of the (110) orthorhombic reflection at $d = 4.08$ Å, at ∼60 °C, with the concomitant appearance of the (100) monoclinic reflection at $d = 4.37$ Å. Since the total area under the existing orthorhombic and monoclinic reflections stays constant, this suggests a solid to solid transformation from the orthorhombic to the monoclinic form.

If one considers the ratio of the $d$-spacings of the two new reflections (4.19 Å/3.78 Å ≈ 1.108) and compares their intensities, it can be concluded that this phase resembles an orthorhombic phase (for linear polyethylene, $d_{110\ \mathrm{ortho}}/d_{200\ \mathrm{ortho}} \approx 1.111$). However, the $d$ values for the new reflections are higher than the conventional $d$ values for the orthorhombic phase and do not match exactly with the known triclinic phase in linear polyethylene. Keeping this in mind and assuming no change along the $c$-axis, the unit cell dimensions for the new orthorhombic phase at 3.8 kbar and room temperature (25 °C) were calculated to be $a = 7.56$ Å, $b = 5.03$ Å, and $c = 2.55$ Å with a unit cell volume of approximately 96.97 Å$^3$ and a density 960 kg/m$^3$. Compared to the conventional orthorhombic phase, the density of the new orthorhombic phase is rather low; i.e., the unit cell is more open (for comparison see Figure 5). In view of the low density of the new orthorhombic phase, we assign this phase as the open-orthorhombic phase in the ethylene−1-octene copolymers. It is to be noted that for the same pressure and temperature the density of the conventional orthorhombic phase increases to a value

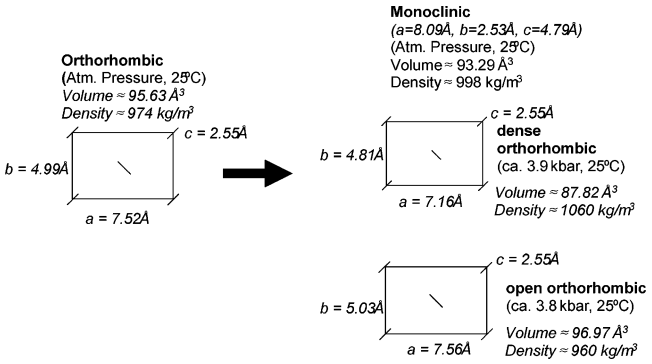


**Figure 5.** Comparison of the lattice parameters obtained from the room temperature WAXD patterns for ethylene−1-octene copolymer (5.2 mol %) at atmospheric and elevated pressures. The differences in the densities of the phases are apparent.

of 1060 kg/m$^3$, which is similar to the one measured for the butyl-branched alkanes crystallized under the similar conditions.[14]

A significant difference in the experimental observations is that the new reflection in the ethylene−1-octene copolymers is much more intense than that of the new reflection in butyl-branched alkanes. The absence of the second reflection in butyl-branched alkanes may simply be explained by the relatively low intensity of the first reflection. In this perspective the open-orthorhombic phase in ethylene−octene copolymers is likely to have the same origin as the assigned pseudohexagonal phase in butyl-branched alkanes and thus is likely to arise by crystallization of the interphase with a crystallographic registration determined by the parent crystal. In the branched copolymers we have so far considered, the crystal fold surface is decorated with hexyl, butyl, or methyl branches that cannot be incorporated within the apparent crystal lattice. Pressure facilitates segregation of equal ethylene sequence lengths in the homogeneous copolymers and thus promotes cocrystallization of the chains and branches that are organized at the interphase and the crystal surface, respectively. Thus, when given the appropriate crystallization conditions, crystallization is not restricted to the interphase alone but instead can extend further beyond the original crystalline domains into the amorphous region as is revealed by the high intensity of the new reflections. Crystallization of the amorphous phase can occur only if the chain folds back into the crystal by adjacent reentry, due to the branch remaining at the fold surface because of its length. The separation of the branches is dictated by the fold to provide the experimentally observed open-orthorhombic reflections, which in turn should have the same crystal form as their parent ethylene sequence lengths.

Two processes occurring in Figure 4a must be highlighted further: (a) starting from the orthorhombic phase the reflections associated with the open-orthorhombic phase appear, and (b) after the appearance of this open orthorhombic phase, the monoclinic phase comes in with a concomitant contraction and decrease in the intensity of the original orthorhombic lattice. This has also been observed in butyl-branched alkanes (Figure 1a).

A plausible explanation of the observed sequence mentioned above can be as follows:

(i) A lattice mismatch with the parent orthorhombic phase will occur with crystallization of the interphase and the amorphous component associated with it in the open-orthorhombic form.

(ii) Since the volume of the interphase will decrease upon crystallization, a uniaxial stress will develop at the crystal surface, and initially, the crystals can accommodate the strain developed. Upon further increasing the pressure, we have shown that the open-orthorhombic phase does not compress, whereas the parent orthorhombic phase does show compression. This increasing stress must be relieved by shear within the bulk of the crystal, causing the majority of crystals to transform from the parent orthorhombic to the monoclinic phase.

(iii) As the stress will be localized within the interphase of the individual crystals no macroscopic orientation will be anticipated.

(iv) The solid−solid transformation from orthorhombic to monoclinic phase is a nucleation-dependent process above a critical strain; because of this kinetic reason, the monoclinic phase follows, rather than appears simultaneously, with the open-orthorhombic phase.

(v) This transformation is likely to be surface to volume dependent (crystal size). Since in the sample a broad distribution of crystal sizes is anticipated, the larger crystals are likely to retain orthorhombic packing, whereas the majority of crystals will transform into the monoclinic phase, with a contracted lattice in order to accommodate the lattice mismatch.

We would like to add that the origin of the transformation of the orthorhombic phase into the monoclinic form is of particular interest, not just in these samples but also in linear polyethylenes where it is also observed.

The decrease in the surface free energy is a requisite in crystallization. In polymers this is ideally achieved by the formation of extended chain crystals. Such a possibility cannot arise in branched polymers, where the branches are to be excluded from the lattice. Our experimental data suggest that, in such a class of polymers, crystals having an ordered interphase will be the thermodynamically stable state that could be ultimately obtained by adjacent reentry on the crystal surface. The principal difference between the branched alkanes and the ethylene−1-octene copolymers will be the amount of material bound to the parent crystal that can crystallize due to the structural order that arises at elevated pressure−temperature. It should be remembered that in butyl-branched alkanes the branches occur at exactly half the chain length. For this reason, the amount of amorphous component associated with the crystal will be less than that inherent in the ethylene-1-octene copolymers where the equal length branches are distributed inhomogeneously along the main chain. Therefore, the amount of material that can crystallize in the open-orthorhombic phase, upon providing the necessary pressure−temperature cycle, will be greater for the ethylene-1-octene copolymers.

Upon the release of pressure, the (100) monoclinic reflection moves toward lower angles and disappears at ∼1.7 kbar (Figure 6). The reflection at 3.99 Å assigned to the dense (110) orthorhombic lattice also shifts to lower angles implying an expansion of the lattices on releasing pressure, whereas the (110) open-orthorhombic reflection hardly changes its $d$ value from 4.19 Å. The dense orthorhombic reflection merges with the (110) reflection of the open-orthorhombic phase at ∼2.7 kbar, resulting in a single reflection. This single reflection

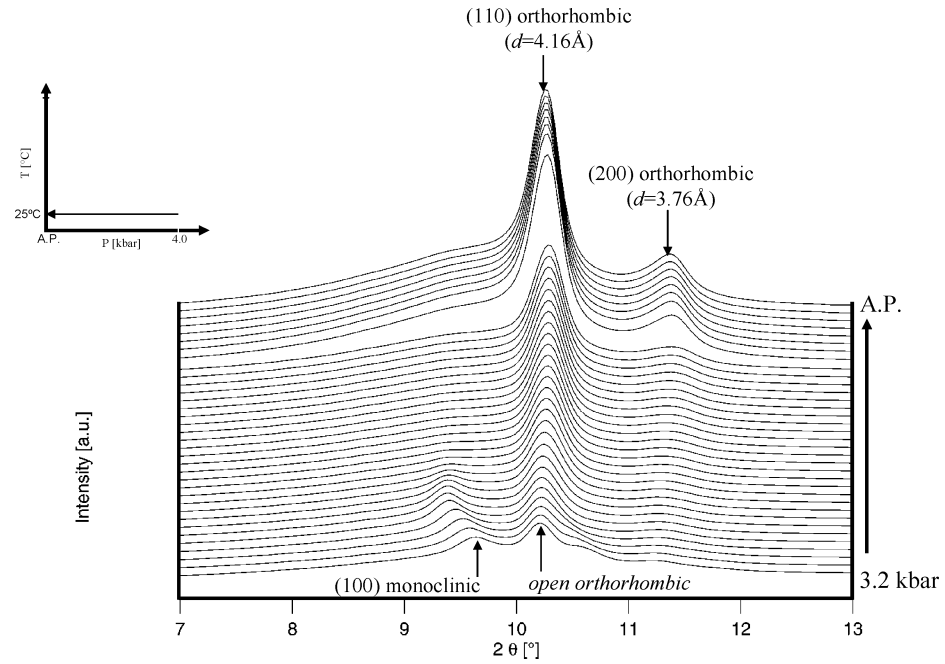


**Figure 6.** WAXD integrations recorded during pressure release from 4 kbar at room temperature for ethylene−1-octene copolymer obtained after the pressure−temperature cycle applied in Figure 4. While monoclinic and orthorhombic reflections shift the open-orthorhombic reflection merges with the parent orthorhombic phase. At this point no shift in the monoclinic phase is observed on the further release of pressure. The monoclinic reflection disappears at lower pressures. These observations on the copolymer are similar to that in butyl-branched alkanes crystallized under the similar conditions (see Figure 1b).

shifts, but very gradually, to lower $d$ values and attains a Bragg $d$ value of 4.16 Å at atmospheric pressure; i.e., it returns to the lattice spacing of the (110) orthorhombic reflection observed earlier for the same ethylene−1-octene copolymer at atmospheric pressure. It is to be noted that this $d$ value of the orthorhombic phase at atmospheric pressure is similar to the open-orthorhombic phase in the compressed state (4.19 Å). Therefore, the positions of the reflections for the open-orthorhombic phase are hardly altered with the application of pressure. The monoclinic phase transforms into the orthorhombic phase. These observations are in agreement with butyl-branched alkanes, where on releasing or increasing pressure no shift in the pseudohexagonal phase was observed (Figure 1a).

To confirm the crystallographic changes occurring, pressure was increased once more at room temperature. Figure 7a shows WAXD patterns recorded during the consecutive increase of pressure at room temperature. With increasing pressure the (110) reflection for the orthorhombic phase again splits into two distinct reflections, $d$ = 4.19 Å (open-orthorhombic phase) and $d$ = 3.99 Å (dense-orthorhombic phase) together with the appearance of the monoclinic phase. A simultaneous split in the (200) reflection of the orthorhombic phase is also observed. The intensity of the dense-orthorhombic reflection $d$ = 3.99 Å decreases with the appearance of the (100) monoclinic reflection ($d$ = 4.48 Å). From the figure it is evident that the intensity and position of the open-orthorhombic reflection remain unchanged. These observations are in agreement with crystallization from the melt at elevated pressures (Figure 4a). Comparison of Figure 3a with Figure 7a shows a clear distinction in the compression behavior of samples crystallized from the melt at atmospheric and elevated pressures. Obviously the morphology of the same material for the two starting conditions is distinctly different, though the degree of crystallinity and size of crystalline and amorphous components remain the same (manuscript in preparation). The sample crystallized at the elevated pressures has an organized interphase and amorphous component whereas no such organization is anticipated in the sample crystallized at atmospheric pressure. On compression, the sample crystallized at atmospheric pressure shows a loss in crystallinity and a transformation of a considerable amount of the orthorhombic phase into the monoclinic phase (Figure 3a). The origin of the monoclinic phase in this figure can be understood by considering the higher compressibility of the amorphous phase compared to the orthorhombic phase. This inhomogeneous distribution of compressibility within the sample results in a localized shear stress that crystals relieve by transformation into the monoclinic phase without showing any orientation by X-ray diffraction.

Figure 7b shows the Raman spectra of the sample crystallized from the melt at elevated pressures. Room temperature spectra of the sample were recorded at atmospheric and elevated pressures (3.9 kbar). The pressure-crystallized sample exhibits a different behavior on compression compared to the sample crystallized at atmospheric pressure (Figure 3b): the intensity of the 1415 $cm^{-1}$ peak is almost constant at 3.9 kbar and does not decrease during compression. Although, a broadening of the band occurs in the methylene bending region (1400−1500 $cm^{-1}$), the crystal field splitting (band at 1440 $cm^{-1}$) is still visible. This suggests that the packing of the chains in the orthorhombic unit cell is maintained at 3.9 kbar and emphasizes the stability of crystals obtained upon pressure crystallization. These observations are in accordance with the WAXD patterns. Since no changes in the two trans peaks at 1060 and 1130 $cm^{-1}$ are seen, this suggests that the planar zigzag conformation is maintained.

To explore the stability of different phases, the sample thus crystallized at elevated pressure−temperature (i.e., the sample from Figure 7a) was heated isobarically at 3.9 kbar. Figure 8 shows WAXD patterns recorded during heating of the sample. The reflection assigned

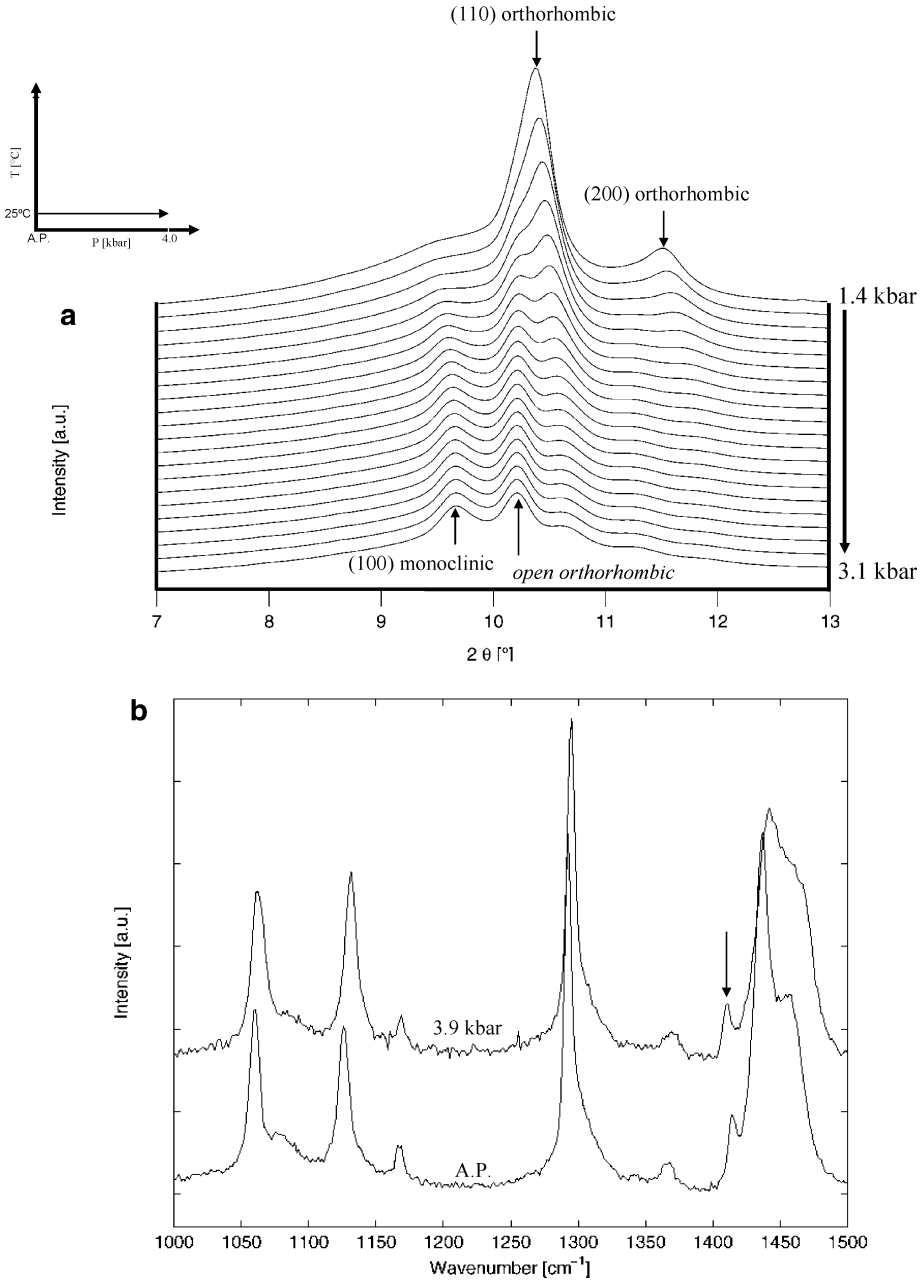


**Figure 7.** (a) Diffraction patterns of the crystalline sample obtained from Figure 6 during the increase in pressure from 1.4 to 3.1 kbar at room temperature, i.e., for a previously pressure-crystallized sample. This shows the reappearance of the monoclinic after change of the (110) orthorhombic reflection into a dense and an open-orthorhombic phase. (b) Room temperature Raman spectrum of the ethylene−1-octene copolymer following the same pressure−temperature treatment. No significant loss in intensity of the 1415 $cm^{-1}$ band upon pressurizing the crystalline sample is observed. Comparison with Figure 3b shows a clear distinction in the behavior of the sample previously crystallized at atmospheric pressure.

to the open-orthorhombic phase disappears at temperatures as low as 110 °C, leaving behind the dense orthorhombic and monoclinic phase. No change in the intensity of the two reflections is observed with the disappearance of the open-orthorhombic phase. On heating further, the (100) monoclinic reflection disappears at approximately 140 °C, and the intensity of the orthorhombic reflection increases. This suggests a solid−solid transformation of the crystals from the monoclinic to the orthorhombic phase. The crystals now in the orthorhombic phase melt at approximately 200 °C. It is to be noted that the open-orthorhombic phase melts much earlier than the monoclinic phase though the former crystallizes at higher temperatures (lower supercoolings) than the monoclinic phase. This suggests a metastable nature of the component crystallized in the open-orthorhombic phase. Although the structure at the interphase disappears since the open-orthorhombic reflections disappear, the monoclinic phase remains because of the thermodynamic stability of the crystals.

Since the change in the specific volume of the sample on increasing or decreasing pressure is the same as decreasing or increasing temperature, we can directly compare Figure 1b for butyl-branched alkanes with Figure 8 for the ethylene−1-octene copolymer. The same general behavior is seen with the solid−solid transformation of monoclinic phase to orthorhombic phase being observed after the disappearance of the "pseudohexagonal" or "open-orthorhombic" reflections. This behavior

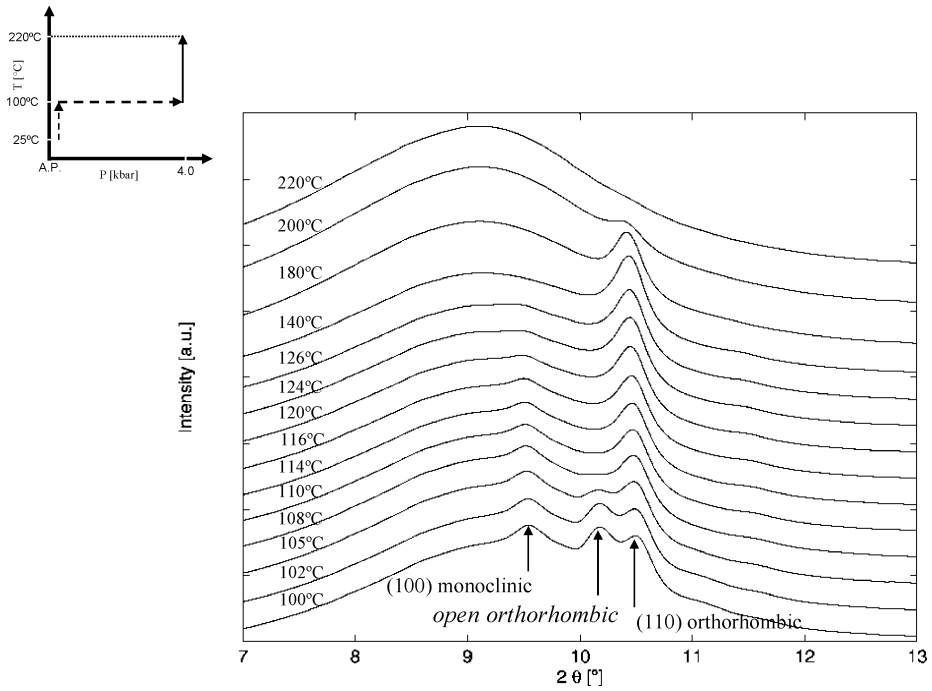


**Figure 8.** WAXD integrations for the sample resulting from Figure 7 as a function of temperature during heating at a pressure of ~3.9 kbar. The open-orthorhombic phase melts at approximately 110 °C whereas the monoclinic reflection disappears around 126 °C. With disappearance of the monoclinic phase the intensity of the orthorhombic reflection increases.

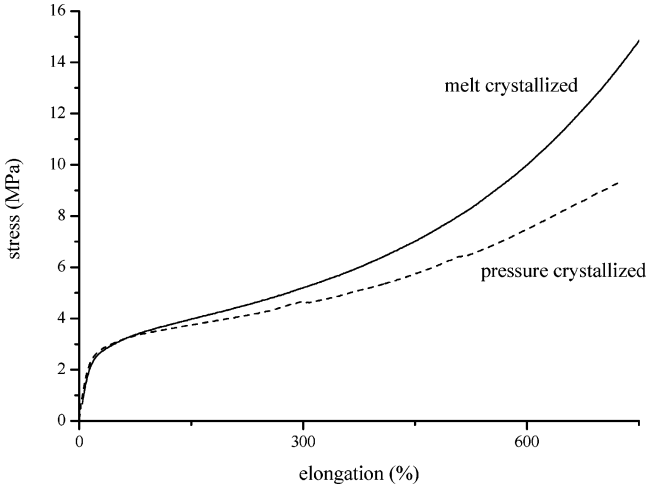


**Figure 9.** Stress−strain curves for samples crystallized upon cooling at atmospheric and elevated pressures. These experiments were performed at room temperature and reveal the same modulus and yield point but differences in the strain-hardening. Each line is the average of four separate measurements.

must be general for these types of polymers where the branches cannot be included in the crystalline lattice.

We stated earlier that to minimize the surface free energy the branched polymers would tend to disentangle and form a well-defined interphase and structured amorphous region associated with it through adjacent reentry. This would promote crystallographic registration of the chains at the interphase and the amorphous region. If such a situation exists, disentangled crystals will be formed which would exhibit differences in the macroscopic deformation. Figure 9 shows a stress−strain curve of two sets of samples—one crystallized at atmospheric pressure and the other at elevated pressures under the conditions described in the experiments above. Compression tests were also performed to reveal the intrinsic behavior of the two samples. Both tensile and compression tests show the same modulus and yield point for the two sets of samples, suggesting a similar degree of crystallinity. However, a remarkable difference in the strain hardening of the two materials is observed. The polymer crystallized at atmospheric pressure shows a higher slope in strain hardening compared to the sample crystallized at elevated pressures. Since the slope in strain hardening is associated with the number of entanglements,[22,23] this clearly shows that the amorphous region of the sample crystallized under pressure possesses remarkably fewer entanglements compared to the sample crystallized at atmospheric pressure. These observations are in agreement with the requisite for structural ordering of the chains at the crystal surface as can be achieved through adjacent reentry.

## Conclusions

From our work on branched polymers we can conclude the following:

1. Pressure facilitates the disentanglement process even though the highly mobile hexagonal phase does not feature in the crystallization of the branched polyethylenes.

2. When given the appropriate conditions for crystallization, chains in the interphase between the crystalline and amorphous regions will tend to organize and show crystallographic registration. This can only occur if there is adjacent reentry. This means that the amorphous region associated with the interphase will also tend to organize. Furthermore, it is clear that, under these conditions, the structural organization can extend further from the crystal surface than the predicted 6−7 Å normally quoted for the interphase. This appears to be the thermodynamically stable state for these branched polymers that cannot form extended chain crystals.

3. The origin of the monoclinic phase appears to be the localized relaxation of the shear stress that builds

up with crystallization of the interphase under compression. This seems to be a general phenomenon that one may encounter during application of pressure in polyethylenes, both linear and branched.

4. The stability of the crystals under compression is strongly dictated by the crystallization conditions. For example, samples crystallized at atmospheric pressure show a considerable loss in crystallinity upon increasing pressure whereas the samples crystallized at elevated pressures show crystallization of the structured region on the crystal surface and successive transformations without any loss in crystallinity.

5. The structural organization at the interphase through the application of pressure influences the mechanical behavior of the polymer, hence revealing the disentanglement process during crystallization at elevated pressures.

**Acknowledgment.** Experimental support provided by the Materials Science beamline, ID11, of ESRF (Grenoble) is gratefully acknowledged. The authors thank Dutch Polymer Institute for the financial support.

## References and Notes

(1) Brooke, G. M.; Burnett, S.; Mohammed, S.; Proctor, D.; Whiting, M. C. *J. Chem. Soc., Perkin Trans. 1* **1996**, 1635.
(2) Flory, P. J. *Principles of Polymer Chemistry*; Cornell University Press: Ithaca, NY, 1953.
(3) Mandelkern, L. *An Introduction to Macromolecules*; Springer-Verlag: New York, 1983.
(4) Mandelkern, L. *Crystallization in Polymers*; McGraw-Hill Book Co.: New York, 1983.
(5) Keller, A. *Philos. Mag.* **1957**, *2*, 1171.
(6) Heck, B.; Hugel, T.; Iijima, M.; Sadiku, E.; Strobl, G. *New J. Phys.* **1999**, *1*, 17.
(7) Mandelkern, L. *Chemtracts (Macromol. Chem.)* **1992**, *3*, 347−375.
(8) Baker, A. M. E.; Windle, A. H. *Polymer* **2002**, *42*, 667.
(9) Balijepalli, S.; Rutledge, G. C. *J. Chem. Phys.* **1998**, *109*, 6523.
(10) Bassett, D. C. *The Crystallization of Polyethylene at High Pressures*; *Developments in Crystalline Polymers*; Applied Science: London, 1982; pp 115−151.
(11) Bassett, D. C.; Khalifa, A.; Turner, B. *Nature* (*London*) **1972**, *239*, 109.
(12) Rastogi, S.; Hikosaka, M.; Kawabata, H.; Keller, A. *Macromolecules* **1991**, *24*, 6384.
(13) Parker, J. A.; Bassett, D. C.; Olley, R. H.; Jaaskelainen, P. *Polymer* **1994**, *35*, 4140.
(14) Rastogi, A.; Hobbs, J. K.; Rastogi, S. *Macromolecules* **2002**, *35*, 5861.
(15) Hay, I. L.; Keller, A. *J. Polym. Sci., Part C* **1970**, *30*, 289.
(16) Litvinov, V. M.; Mathot, V. B. F. *Solid State Nucl. Magn. Reson.* **2002**, *22*, 218.
(17) Vanden Eynde, S.; Mathot, V. B. F.; Hoehne, G. W. H.; Schawe, J. W. K.; Reynaers, H. *Polymer* **2000**, *41*, 3411.
(18) Hikosaka, M.; Seto, T. *Jpn. J. Appl. Phys.* **1982**, *21*, L332.
(19) Rastogi, S.; Newman, M.; Keller, A. *Nature (London)* **1991**, *353*, 55. Rastogi, S.; Newman, M.; Keller, A. *J. Polym. Sci., Part B: Polym. Phys.* **1993**, *31*, 125. Rastogi, S.; Hoehne, G. W. H.; Keller, A. *Macromolecules* **1999**, *32*, 8897. Van Ruth, N. J. L.; Rastogi, S. *Macromolecules*, in press.
(20) Strobl, G. R.; Hagedorn, W. *J. Polym. Sci., Polym. Phys. Ed.* **1978**, *16*, 1181.
(21) Kurelec, L.; Rastogi, S.; Meier, R. J.; Lemstra, P. J. *Macromolecules* **2002**, *33*, 5593.
(22) Lemstra, P. J.; Bastiaansen, C. W. M.; Rastogi, S. Basic Aspects of Solution (Gel) Spinning and Ultra-Drawing of Ultrahigh Molecular Weight Polyethylene. In *Structure Formation in Polymeric Fibres*; Salem, D. R., Ed.; 2002.
(23) Schrauwen, B. A. G.; Janssen, R. P. M.; Govaert, L. E.; Meijer, H. E. H. *Macromolecules* **2004**, *37*, 6069.

MA048023B